

ON THE DETERMINATION OF THE ZnAs_2 BAND STRUCTURE PARAMETERS

V. A. Morozova, S. F. Marenkin, and O. G. Koshelev

A method for taking into account light scattering in ZnAs_2 and obtaining the $\alpha^{\parallel}(h\nu)$ absorption spectrum was suggested. At the $\mathbf{E} \parallel \mathbf{c}$ polarization, the absorption edge was shown to be determined by indirect and direct allowed transitions with the energy difference 64 meV between them, which involved exciton states. For both transitions, in the temperature range 80–300 K, the forbidden band width was determined.

The ZnAs_2 semiconducting compound of the A^2B^5 group crystallizes in the monoclinic system. The presence of chain structures formed by As atoms and extended along the c -axis determines substantial anisotropy of the optical and electric properties of zinc diarsenide. Calculations of the band structure parameters of ZnAs_2 are impeded by the large number of atoms in the unit cell [1, 2]. These parameters can be determined by experimentally studying the spectra of optical absorption $\alpha(h\nu)$, photoconductivity, and short-circuit photocurrent (SCPC). The $\alpha(h\nu)$ spectra are calculated from the $T(h\nu)$ transmission spectra by the formula

$$T = \frac{(1 - R)^2 \exp(-\alpha d)}{1 - R^2 \exp(-2\alpha d)}, \quad (1)$$

where T , α , and R are the transmission, absorption, and reflection coefficients, respectively; and d is the sample thickness. The $T(h\nu)$ spectra at 300 K were reported in [3], and the $\alpha(h\nu)$ spectra at 300 and 80 K in [4]. It was shown that the α value and the energy corresponding to the fundamental absorption edge depended on the orientation of the \mathbf{E} electric field vector of the incident wave with respect to the c -axis of the crystal. According to [1-4], ZnAs_2 is a straight-band semiconductor with the forbidden band width $\varepsilon_g^d(\mathbf{E} \parallel \mathbf{c}) \cong 0.90$ eV and $\varepsilon_g^d(\mathbf{E} \perp \mathbf{c}) \cong 0.93$ eV at 300 K. In the photon energy range $h\nu = 0.5\text{--}0.86$ eV, the special features of the $T(h\nu)$ spectra (the T^{\perp} value was constant, while the T^{\perp}/T^{\parallel} ratio changed from 1.4 to 1.7 [3]) were not explained. In [4], these observations were attributed to impurity absorption to get $\alpha_0^{\perp} \cong 2.3$ cm⁻¹ and $\alpha_0^{\parallel} \cong 18$ cm⁻¹ at $h\nu = 0.8$ eV.

Owing to advances in growing the ZnAs_2 single crystals [5], the level of their impurity absorption was decreased to $\alpha_0 \leq 0.1$ cm⁻¹. Samples of this material of thickness $d \leq 0.3$ cm ($\alpha d \ll 1$) were transparent in the range $h\nu = 0.5\text{--}0.86$ eV, and the T coefficient had to be constant, as was observed for $T^{\perp} \cong 0.5$. The T^{\parallel} coefficient, however, depended on $h\nu$ and d . We showed in [6] that, at $\mathbf{E} \parallel \mathbf{c}$, light propagation had special features determined by spatial inhomogeneities of the refraction index sensitive to light polarization. This circumstance was overlooked in [4], which led to overestimated α^{\parallel} values.

In A^2B^5 compounds, different ε_g values are observed for $\mathbf{E} \perp \mathbf{c}$ and $\mathbf{E} \parallel \mathbf{c}$ due to splitting of the valence band top at $k = 0$ under the action of crystal field [1, 2]. The reflectance and photoconductivity spectra measured with $\mathbf{E} \perp \mathbf{c}$ and $\mathbf{E} \parallel \mathbf{c}$ contained peaks assigned to exciton ground states, which made it possible to determine the splitting $\Delta = 20$ meV at 300 K [4, 7]. However, according to [8], ZnAs_2 exhibits only a single exciton series whose $n = 1, 2$ states are observed at 4.2 K in the $\mathbf{E} \parallel \mathbf{c}$ reflectance and $T^{\perp}(h\nu)$

transmission spectra; that is, $\Delta = 0$. Because of intense absorption, exciton peaks are indiscernible in the $T^{\parallel}(h\nu)$ spectra. It may well be that studies of the photoconductivity and short-circuit photocurrent spectra will make it possible to observe them and determine Δ and $\epsilon_g^d(\mathbf{E} \parallel \mathbf{c})$.

In this work, we studied optical transitions in ZnAs₂ near the fundamental absorption edge by the optical transmission, photoconductivity, and short-circuit photocurrent methods to determine the most important band structure parameters.

EXPERIMENTAL

The $T(h\nu)$, photoconductivity, and short-circuit photocurrent spectra were studied in the temperature range 80–300 K in plane-polarized light at $h\nu = 0.5$ –1.1 eV. The c -axis of the crystal always lies in the plane of the plates. The short-circuit photocurrent spectra were recorded with the use of Schottky diodes by the compensation method described in [9]. A light beam from an IKS-21 unit (the image of the exit slit of the monochromator) was focused on a ZnAs₂ plate. The light intensity ratio $T_{\text{exp}} = I_1/I_0$ between the beams that reached a photoresistor in the presence I_1 and absence I_0 of a plate was measured. Usually, the light beams had equal apertures, and $T_{\text{exp}} = T$; the α values were then calculated by (1). At $\mathbf{E} \parallel \mathbf{c}$, the aperture, however, depended on the measurement conditions, and $T_{\text{exp}}^{\parallel} \neq T^{\parallel}$ [6]. The $T(h\nu)$ spectra were measured for 11 samples with d of 0.005 to 0.3 cm. In the $h\nu = 0.5$ –0.86 eV range, the samples were transparent, and $T_{\text{exp}}^{\perp} = 45$ –50% at all $h\nu$; according to [6], $T^{\parallel} = 0.95T^{\perp}$ because of anisotropy of R . These T^{\perp} values were used to determine the R^{\perp} coefficients. The R value was sensitive to the state of the surface and changed as time passed; for this reason, it was determined in each series of measurements. To take into account changes in R caused by an increase in α , the reflectance spectra of ZnAs₂ of [7] were used.

RESULTS AND DISCUSSION

The $T_{\text{exp}}^{\perp}(h\nu)$ and $T_{\text{exp}}^{\parallel}(h\nu)$ spectra obtained at 300 K for samples of different thicknesses prepared from the same initial sample by successive grinding are shown in Fig. 1. In the $h\nu = 0.5$ –0.89 eV range, T_{exp}^{\perp} equals 0.5 and does not depend on $h\nu$ and d : all points fall onto curve 1; that is, the samples are transparent, and $T_{\text{exp}}^{\perp} = T^{\perp}$. At $\mathbf{E} \parallel \mathbf{c}$, a transparency region is only observed for samples with $d \leq 0.02$ cm (curve 2), for which $T_{\text{exp}}^{\parallel} = T^{\parallel}$. At $h\nu > 0.87$ eV, fundamental absorption causes T^{\perp} and T^{\parallel} (curves 1, 2) to decrease as $h\nu$ and d increase (αd grows); the α^{\perp} and α^{\parallel} values are then calculated by (1).

In the $h\nu = 0.5$ –0.86 eV range, samples with $d > 0.02$ cm show an exponential decrease in $T_{\text{exp}}^{\parallel}$ (curves 4, 3) as $h\nu$ and d increase [6]. The $T^{\parallel}(h\nu)$ spectra are then calculated with an $A(h\nu, d)$ coefficient taking into account light losses. This coefficient is determined by extrapolating the $T_{\text{exp}}^{\parallel}(h\nu)$ dependences from the $h\nu = 0.5$ –0.86 eV range to $h\nu > 0.86$ eV (the $T_{\text{extr}}^{\parallel}$ dependences are shown by dashed lines 4, 3), where $T_{\text{exp}}^{\parallel}$ decreases as a result of light scattering and fundamental absorption. We can then write $T^{\parallel}(h\nu) = AT_{\text{exp}}^{\parallel}(h\nu)$, where $A = 0.95T_1^{\perp}/T_{\text{exp}}^{\parallel}(h\nu)$ for $h\nu < 0.86$ eV and $A = 0.95T_1^{\perp}/T_{\text{extr}}^{\parallel}(h\nu)$ for $h\nu > 0.86$ eV (T_1^{\perp} is the T^{\perp} value in the transparency region). The $T^{\parallel}(h\nu)$ spectra of all samples calculated with coefficients A coincide in the $h\nu = 0.5$ –0.86 eV range; at $h\nu > 0.86$ eV, the behavior of the spectra is determined by fundamental absorption only. The described procedure was applied to calculate the $T^{\parallel}(h\nu)$ spectra of all samples with $d > 0.02$ cm; the α^{\parallel} value was then calculated by (1). The spread of the α^{\parallel} values obtained for different samples did not exceed 7%.

Shown in Fig. 2 are the $\alpha(h\nu)$ spectra (solid curves) at 300 K and 80 K for $\mathbf{E} \parallel \mathbf{c}$ and $\mathbf{E} \perp \mathbf{c}$. Because of the presence of a forbidden direct transition at $\mathbf{E} \perp \mathbf{c}$, the $\alpha^{\perp}(h\nu)$ spectra (curves 2, 4) contain exciton absorption peaks. Earlier [10], we studied the $T^{\perp}(h\nu)$ spectra at 5–10 K; we observed the structure corresponding to free exciton states with $n = 1, 2, 3$ and determined the exciton bond energy $G = 17.5$ meV and $\epsilon_g^d(\mathbf{E} \perp \mathbf{c})$ at 5–300 K. In [8], the value $G = 12$ meV was obtained.

Figure 2 shows that the $\alpha(h\nu)$ spectra for $\mathbf{E} \parallel \mathbf{c}$ at $\alpha < 10$ cm⁻¹ have the shape typical of indirect transitions (curves 1, 3). This figure also contains the photoconductivity (5, 6) and short-circuit photocurrent spectra (7, 8) recorded under similar conditions and, in order that the spectra may conveniently be compared, shifted along the axis of ordinates to coincidence with the $\alpha(h\nu)$ spectra in the region of small α values. One can see that the shifted spectra coincide with $\alpha(h\nu)$ over a substantial

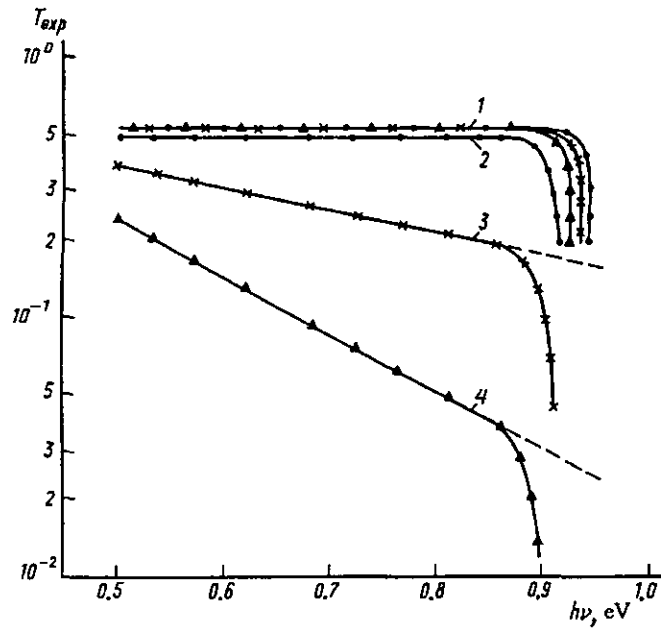


Fig. 1

Optical transmission spectra for $E \perp c$ at $d = 0.02$ – 0.29 cm (1) and $E \parallel c$ at $d = 0.29$ (4), 0.11 (3) and 0.02 cm (2).

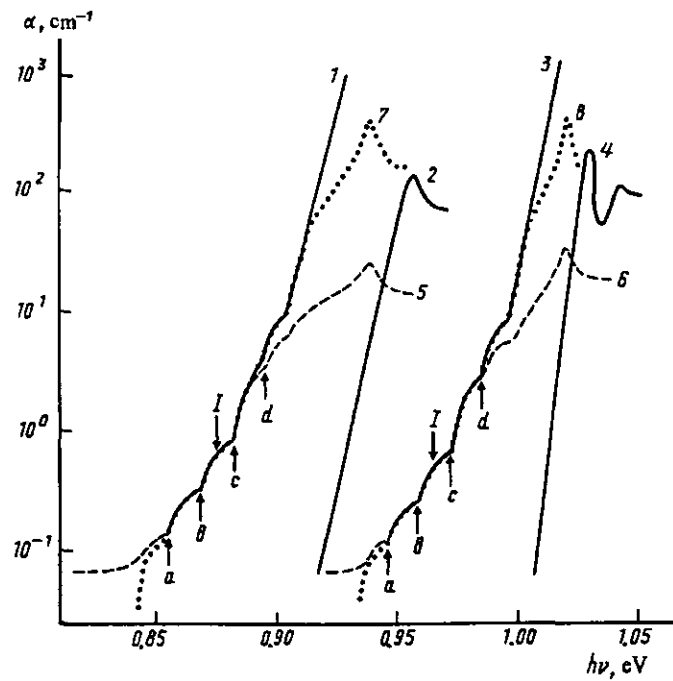


Fig. 2

Fundamental absorption (1-4), photoconductivity (5, 6), and short-circuit photocurrent spectra (7, 8) for $E \parallel c$ (1, 3, 5-8) and $E \perp c$ (2, 4) at 300 K (1, 2, 5, 7) and 80 K (3, 4, 6, 8).

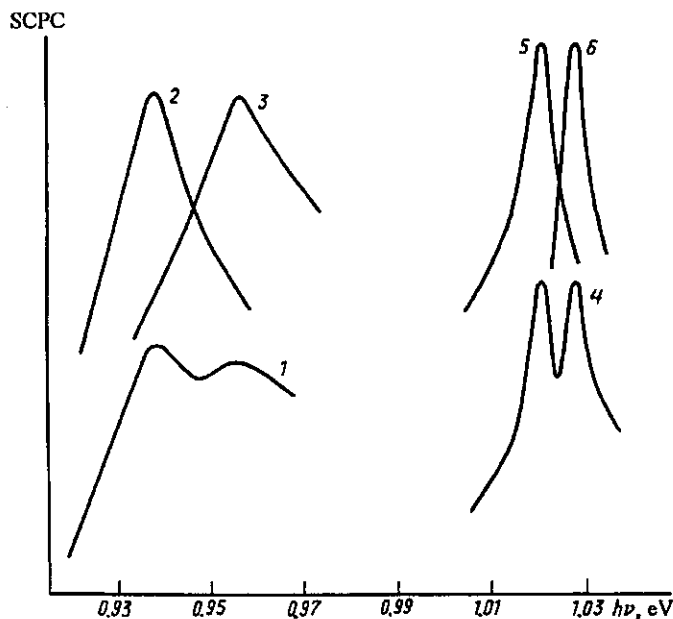


Fig. 3

Short-circuit photocurrent spectra in nonpolarized light (1, 4), at $E \parallel c$ (2, 5), and $E \perp c$ (3, 6) recorded at 300 (1-3) and 80 K (4-6).

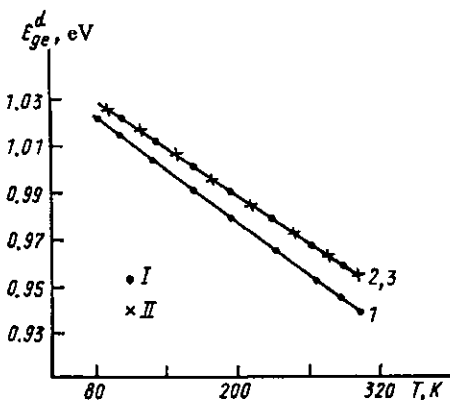


Fig. 4

Temperature dependences of $\epsilon_{ge}^d(E \parallel c)$ (1) and $\epsilon_{ge}^d(E \perp c)$ (2, 3) (I denotes short circuit photocurrent spectra, and II absorption spectra).

range of α values. Such a coincidence is to be expected, because the photoconductivity is proportional to $\alpha(h\nu)$ at $\alpha d \ll 1$, and the short-circuit photocurrent is proportional to $\alpha(h\nu)$ at $\alpha L \ll 1$, where L is the diffusion length of minority carriers [11]. The wide range of α values at which the $\alpha(h\nu)$ and short-circuit photocurrent spectra coincide implies that $L \ll d$. The thresholds of the short-circuit photocurrent spectra (curves 7, 8) are observed at smaller α values than those of the photoconductivity spectra (5, 6) due to impurity absorption, which makes no contribution to the short-circuit photocurrent signal. Our study of the photoconductivity and short-circuit photocurrent spectra substantiated the conclusion that the fundamental absorption edge of $ZnAs_2$ is determined by an indirect transition. The inflection points denoted by a, \dots, d in Fig. 2 are the boundaries of the participation (absorption or emission) of phonons of various energies

($k\theta_m$) in light absorption. A decrease in temperature causes the spectra to shift to larger $h\nu$ values while retaining their main features. Being an indication of the participation of the same set of phonons in the indirect transition at 80–300 K, this allowed us to determine the temperature shift coefficient for $\varepsilon_g^i(\mathbf{E} \parallel \mathbf{c})$ from the temperature-induced shift of an arbitrary inflection point, $\beta^i(\mathbf{E} \parallel \mathbf{c}) = (-4.3 \pm 0.2) \times 10^{-4}$ eV/K.

An analysis of the $\alpha^{\parallel}(h\nu)$ spectra according to Elliott [12] showed that the indirect transition is allowed and involves exciton states. The $\alpha^{\parallel}(h\nu)$ spectra can be used to determine the exciton forbidden band width, $\varepsilon_{ge}^i = (\varepsilon_g^i - G)$, provided the thresholds corresponding to absorption and emission of a phonon of a certain energy are correctly identified. According to [12], such thresholds are situated symmetrically with respect to ε_g^i and are separated by a $2k\theta_m$ energy range. The photoluminescence spectra of ZnAs₂ at 80 K contained an emission band of an unknown nature with a maximum at $h\nu = 0.965$ eV and a half-width of 25 meV [13]. The shape of the band was characteristic of a radiative recombination indirect transition. It is therefore natural to suggest that, at 80 K, $\varepsilon_{ge}^i(\mathbf{E} \parallel \mathbf{c}) = 0.965$ eV. This value is marked by *I* in Fig. 2 (curve *β*). The energy positions of the *b* and *c* (also *a* and *d*) thresholds are symmetrical with respect to point *I*. At 300 K, $\varepsilon_{ge}^i(\mathbf{E} \parallel \mathbf{c}) = 0.875$ eV (curve *1*). Taking into account that $G = 17.5$ meV, we obtain $\varepsilon_g^i(\mathbf{E} \parallel \mathbf{c}) = 0.892$ eV. The positions of the inflection points and the absorption threshold with respect to $\varepsilon_{ge}^i(\mathbf{E} \parallel \mathbf{c})$ were used to determine $k\theta_1 = 6$ –7 meV, $k\theta_2 = 19$ –20 meV, and $k\theta_3 = 33$ –35 meV. In the far IR region, at $h\nu$ corresponding to the obtained $k\theta_{1-3}$ values, the ZnAs₂ lattice absorption lines were observed [14].

Intense absorption at $\mathbf{E} \parallel \mathbf{c}$ and $\alpha > 10$ cm⁻¹ (see Fig. 2, curves *1*, *β*) is indicative of a direct allowed transition and impedes observation of exciton peaks. The photoconductivity and short-circuit photocurrent spectra in the $h\nu$ region where $\alpha > 10^3$ cm⁻¹ contained absorption peaks (curves *5*–*8*).

Shown in Fig. 3 are short-circuit photocurrent spectrum regions recorded at 300 and 80 K in nonpolarized and polarized light. In nonpolarized light, the spectra contained two peaks, which shifted to larger $h\nu$ values and noticeably narrowed as temperature decreased (curves *1*, *4*). Both peaks are polarized; at $\mathbf{E} \parallel \mathbf{c}$, there remains the long-wave peak (*2*, *5*), and, at $\mathbf{E} \perp \mathbf{c}$, its short-wave counterpart is observed (*3*, *6*); their half-widths are smaller than kT , which is characteristic of exciton absorption.

The temperature dependences of energy positions of these peaks maxima at $\mathbf{E} \parallel \mathbf{c}$ and $\mathbf{E} \perp \mathbf{c}$ and of the $\varepsilon_{ge}^d(\mathbf{E} \perp \mathbf{c})$ exciton peak observed in the $\alpha^{\perp}(h\nu)$ spectra (see Fig. 2) are shown in Fig. 4. The energy positions of the short-wave peak (Fig. 4, curve *2*) and of the ground state ($n = 1$) of the free exciton forbidden series (Fig. 4, curve *3*) coincide. It can therefore be claimed that the absorption peaks observed in the short-circuit photocurrent spectra at $\mathbf{E} \parallel \mathbf{c}$ are caused by the ground state ($n = 1$) of the free exciton allowed series; that is, straight line *1* (Fig. 4) is the temperature dependence of $\varepsilon_{ge}^d(\mathbf{E} \parallel \mathbf{c})$. The slopes of straight lines *1*, *2* were used to determine the coefficients $\beta^d(\mathbf{E} \parallel \mathbf{c}) = (-3.8 \pm 0.1) \times 10^{-4}$ eV/K and $\beta^d(\mathbf{E} \perp \mathbf{c}) = (-3.3 \pm 0.1) \times 10^{-4}$ eV/K. The difference between the β values is indicative of noticeable anisotropy of thermal expansion of the lattice, which is characteristic of A²B⁵ compounds.

We obtained $\Delta = 17 \pm 1$ and 7 ± 0.5 meV and (taking into account G) $\varepsilon_g^d(\mathbf{E} \parallel \mathbf{c}) = 0.956$ and 1.039 eV at 300 and 80 K, respectively.

CONCLUSIONS

The study of combined absorption, photoconductivity, and short-circuit photocurrent data on ZnAs₂ gave new information on the band structure of this compound.

The fundamental absorption edge of ZnAs₂ was shown to be determined by an indirect allowed transition involving exciton states; for this transition, $\varepsilon_g^i(\mathbf{E} \parallel \mathbf{c}) = 0.89$ eV (300 K), and $\beta^i(\mathbf{E} \parallel \mathbf{c}) = (-4.3 \pm 0.2) \times 10^{-4}$ eV/K (80–300 K). The energies of phonons participating in absorption were estimated.

At the $\mathbf{E} \parallel \mathbf{c}$ polarization, there also occurred a direct allowed transition involving exciton states; for this transition, $\varepsilon_g^d(\mathbf{E} \parallel \mathbf{c}) = 0.956$ eV (300 K) and $\beta^d(\mathbf{E} \parallel \mathbf{c}) = (-3.8 \pm 0.1) \times 10^{-4}$ eV/K (80–300 K).

REFERENCES

1. V.B. Lazarev, V.Ya. Shevchenko, Ya.Kh. Grinberg, and V.V. Sobolev, *Semiconducting Compounds of the A^{II}B^V Group* (in Russian), Moscow, 1978.
2. N.N. Syrбу, *The Optoelectronic Properties of A^{II}B^V Compounds* (in Russian), Kishinev, 1983.
3. W.J. Turner, A.S. Fischler, and W.E. Reese, *Phys. Rev.*, vol. 121, no. 3, p. 759, 1961.

4. V.V. Sobolev and N.N. Syrbu, *Phys. Status Solidi*, vol. 51, no. 2, p. 863, 1972.
5. S.F. Marenkin, A.M. Raukhan, D.I. Pishchikov, and V.B. Lazarev, *Izv. Ross. Akad. Nauk, Neorg. Mater.*, vol. 28, no. 9, p. 1813, 1992.
6. V.A. Morozova, S.F. Marenkin, O.G. Koshelev, and A.G. Mironov, *Vestn. Mosk. Univ. Fiz. Astron.*, no. 6, p. 62, 1998.
7. V.V. Sobolev, N.N. Syrbu, and Ya.A. Ugai, *Phys. Status Solidi*, vol. 31, p. 51, 1969.
8. V.V. Sobolev, A.I. Kozlov, S.F. Marenkin, and K.A. Sokolovskii, *Izv. Akad. Nauk SSSR, Neorg. Mater.*, vol. 21, no. 8, p. 1276, 1985.
9. O.G. Koshelev, V.A. Morozova, E.Yu. Barinova, et al., *Vestn. Mosk. Univ. Fiz. Astron.*, no. 4, p. 87, 1993.
10. V.A. Morozova, T.V. Semenenya, S.F. Marenkin, et al., *Vestn. Mosk. Univ. Fiz. Astron.*, no. 5, p. 86, 1996.
11. A.M. Vasil'ev and A.P. Landsman, *Semiconductor Photoconverters* (in Russian), Moscow, 1971.
12. R.I. Elliott, *Phys. Rev.*, vol. 108, no. 6, p. 1384, 1957.
13. S.F. Marenkin, D.I. Pishchikov, V.A. Leont'eva, et al., *Izv. Ross. Akad. Nauk, Neorg. Mater.*, vol. 29, no. 5, p. 607, 1993.
14. J. Wieszka, Z. Mazurak, and D.I. Pishchikov, *Phys. Status Solidi B*, vol. 170, p. 89, 1992.

22 March 1999

Department of Semiconductor Physics